



# Enthalpy of formation of natural hydrous iron phosphate: Vivianite



Lyubov Ogorodova<sup>a,\*</sup>, Marina Vigasina<sup>a</sup>, Lyubov Mel'chakova<sup>a</sup>, Vyacheslav Rusakov<sup>b</sup>,  
Dariya Kosova<sup>c</sup>, Dmitrii Ksenofontov<sup>a</sup>, Igor Bryzgalov<sup>a</sup>

<sup>a</sup> M.V. Lomonosov Moscow State University, Geological Faculty, MSU, Leninskie Gory, 119234 Moscow, Russia

<sup>b</sup> M.V. Lomonosov Moscow State University, Physical Faculty, MSU, Leninskie Gory, 119234 Moscow, Russia

<sup>c</sup> M.V. Lomonosov Moscow State University, Chemical Faculty, MSU, Leninskie Gory, 119234 Moscow, Russia

## ARTICLE INFO

### Article history:

Received 28 October 2016

Received in revised form 20 February 2017

Accepted 22 February 2017

Available online 9 March 2017

### Keywords:

Enthalpy of formation

Tian-Calvet microcalorimetry

Hydrous iron phosphate

Vivianite

## ABSTRACT

This paper presents the new data on thermodynamic properties of hydrous iron phosphate, vivianite. The thermochemical study of natural vivianite  $\text{Fe}_{2.32}^{2+}\text{Fe}_{0.33}^{3+}\text{Mg}_{0.35}(\text{PO}_4)_2(\text{OH})_{0.33}\cdot 7.67\text{H}_2\text{O}$  (Kerch iron ore basin, Republic of Crimea, Russia) was carried out on a high-temperature heat-flux Tian-Calvet microcalorimeter "Setaram" (France). The mineral was characterized by X-ray microprobe analysis, powder and single-crystal X-ray diffraction, thermal analysis, FTIR, Raman and Mössbauer spectroscopy. The value of  $\Delta_f H_m^0(T = 298.15 \text{ K})$  for natural vivianite was found to be  $-(5217 \pm 11 \text{ kJ mol}^{-1})$ . The standard values of the entropy, enthalpy and Gibbs energy of formation at  $T = 298.15 \text{ K}$  for vivianite of theoretical composition  $\text{Fe}_3^{2+}(\text{PO}_4)_2\cdot 8\text{H}_2\text{O}$  were calculated as  $(571.0) \text{ J (K mol)}^{-1}$ ,  $-(5119 \pm 19) \text{ kJ mol}^{-1}$  and  $-(4439 \pm 19) \text{ kJ mol}^{-1}$  respectively.

© 2017 Elsevier Ltd.

## 1. Introduction

Vivianite  $\text{Fe}_3^{2+}(\text{PO}_4)_2\cdot 8\text{H}_2\text{O}$  is the most common stable ferrous iron phosphate. Small amounts of manganese, magnesium and calcium may substitute for iron in the structure. In nature, it occurs in freshwater and marine sediments, in the weathering zone of hydrothermal deposits and pegmatite, it is formed under reducing conditions in siderite sedimentary deposits and in moors, and in sewage sludge. In Russia, the main deposits of vivianite are stratified sedimentary deposits of iron ores of the Kerch Peninsula and Taman Peninsula (Black Sea coast, south of Russia). The mineral crystallizes in the monoclinic system, space group  $C2/m$ . Ferrous ions can occupy two distinct octahedral positions in the structure; in the first position "A" (isolated octahedra) the  $\text{Fe}^{2+}$  is surrounded by four water molecules and two oxygen atoms from  $[\text{PO}_4]^{3-}$  tetrahedra, and in the second position "B" (paired octahedra)  $\text{Fe}^{2+}$  is coordinated to two water molecules and four oxygens from  $[\text{PO}_4]^{3-}$  tetrahedra. Earlier, samples of synthetic and natural vivianite were investigated by various physicochemical methods: powder X-ray diffraction, infrared, Raman and Mössbauer spectroscopy [1–13]. Frost et al. [14] studied the dehydration of vivianite and proposed a model of the process of water removing. It is known that the vivianite crystals extracted from the rock are transparent colorless or light green. In air, their color changes over time

in the indigo-blue due to partial oxidation. The works [14–18] are devoted to the study of the oxidation process of vivianite using Mössbauer, infrared and X-ray photoelectron spectroscopy, thermal and thermogravimetric analysis methods. The chemical formula of the oxidized vivianite as  $\text{Fe}_{3-x}^{2+}\text{Fe}_x^{3+}(\text{PO}_4)_2(\text{OH})_x\cdot (8-x)\text{H}_2\text{O}$  was suggested in Ref. [19]. The mineral with chemical formula  $\text{Fe}^{2+}\text{Fe}_2^{3+}(\text{PO}_4)_2(\text{OH})_2\cdot 6\text{H}_2\text{O}$  was named by the International Mineralogical Association as metavivianite (IMA, 1973-049) [20]. The composition, structure, powder X-ray diffraction, optical properties, density, infrared, Raman and Mössbauer spectra, thermal behavior of metavivianite were studied in Ref. [21].

The information about the thermodynamic properties of vivianite is limited to evaluation given in the paper [22]. In present work, we carried out the first thermochemical study of natural vivianite using a Calvet microcalorimeter and obtained new data on the enthalpy of formation of aqueous iron phosphate.

## 2. Experimental

### 2.1. Materials, equipment and diagnostic methods

The investigation was performed using the natural vivianite (Kerch iron ore basin, Republic of Crimea, Russia) from the collection of the Department of Mineralogy (Geological Faculty of M.V. Lomonosov Moscow State University) (Table 1). The sample was in the form of large, deep blue, prismatic crystals up to 1–1.5 cm

\* Corresponding author.

E-mail address: [logor@geol.msu.ru](mailto:logor@geol.msu.ru) (L. Ogorodova).

**Table 1**  
Provenance and mass fraction purity of substances used in this study.

Substance name	Source	State	Mass fraction purity	Further treatments
Vivianite	Natural (Republic of Crimea, Russia)	Crystal	>0.99 <sup>a</sup>	None
Corundum	Mosreactiv Co., Russia	Crystal	0.999 <sup>b</sup>	None
Platinum	Myprom Co., Russia	Solid	0.999 <sup>b</sup>	None
Lead oxide	Mosreactiv Co., Russia	Powder	0.99 <sup>b</sup>	Melting of the mixture of lead oxide and boric acid in a ratio 2PbO: B <sub>2</sub> O <sub>3</sub> at T = 1073 K
Boric acide	Mosreactiv Co., Russia	Crystal	0.99 <sup>b</sup>	

<sup>a</sup> Purity was estimated according X-ray data.

<sup>b</sup> Purity grade as given by the supplier.

in length. Before the study vivianite was carefully selected by hand picking under a binocular microscope. Detailed diagnostics of mineral was done with use of modern physicochemical methods.

Chemical X-ray microprobe analysis was carried out on a micro-analyzer CAMEBAX SX-50 (Cameca, France). To determine elemental composition, we used the analytical line K $\alpha$  and the following standards: Mg – spinel MgAl<sub>2</sub>O<sub>4</sub>; Ca – perovskite CaTiO<sub>3</sub>; Sr – celestine SrSO<sub>4</sub>; Fe – ilmenite FeTiO<sub>3</sub>; Mn – pyrophanite MnTiO<sub>3</sub>; P – KTiPO<sub>5</sub>. The natural minerals were provided by A.E. Fersman Mineralogical Museum and were tested using standards supplied by company Cameca using the “Camebax SX-50” and a Jeol JSM-6480LV scanning electron microscope equipped with an INCA-Wave 500 wavelength dispersive spectrometer (Jeol, Japan). The mode of operation was as follows: accelerating voltage 15 kV; probe current 30 nA.

The thermal behavior of vivianite was studied using NETZSCH TG 209 F1 (Germany) in the temperature range from room temperature to 873 K under following conditions: heating rate was 10°/min; steam of dry air (oxidative atmosphere) or nitrogen (inert atmosphere) 20 ml/min. The experiment was carried out in a alundum crucible (V = 85 mm<sup>3</sup>, d = 6.8 mm) with pierced lid. The specimen weights (3–7) ( $\pm 2 \times 10^{-2}$ ) mg were determined on an analytical balance A&D GH-202. Calibration technique of the instrument is described in Ref. [23]. NETZSCH Proteus Analysis software was applied to process TGA curves. Experimental and computational procedures for TGA were performed according to standards ISO 11358 and ISO 11357-1.

Powder X-ray analysis was performed on a diffractometer STOE-STADI MP (Germany) equipped with a curved Ge (111) monochromator which gives strictly monochromatic CuK $\alpha$ 1 radiation ( $\lambda = 1.54056 \text{ \AA}$ ). Data were collected in a regime of sequential overlapping of scanned regions using a linear position-sensitive detector with an angle of coverage of 5° at 2 $\theta$  with a channel width of 0.02°. Determination of the phase composition was made using a software package WinXPow [24], program Match! [25] and associated PDF-2 powder database [26]. Single-crystal X-ray study was carried out using an Xcalibur S CCD (Oxford Diffraction) diffractometer with MoK $\alpha$ -radiation.

IR-spectroscopic investigation was done on a Fourier spectrometer FSM-1201 (Russia) at room temperature in the air over the range of wave numbers from 400 to 4000 cm<sup>-1</sup> with a spectral resolution of 2.0 cm<sup>-1</sup>. The accuracy of the determination of the absorption bands frequencies was  $\pm 1 \text{ cm}^{-1}$ . Specimens for the studies were prepared in the form of suspensions of mineral powder in petrolatum oil.

Raman spectroscopic study was carried out on a Raman microscope EnSpectr R532 (Russia) with a diffraction grating (1800 lines/mm) and a spectral resolution of about 6 cm<sup>-1</sup>. The laser radiation wavelength was equal to 532 nm, the laser radiation power on the sample was approximately 15 mW, a single exposure time was 1 s, signal averaging was done using 50 measurements. Spectrum was obtained on a non-oriented single crystal of about 100  $\mu\text{m}$  in size; a diameter of the focal laser spot was approximately 10  $\mu\text{m}$ .

The Mössbauer spectra have been recorded by using a MS1104Em spectrometer of electromechanical-type in the constant acceleration mode with a triangular form of the variation of the Doppler velocity of the source with respect to the absorber. <sup>57</sup>Co nuclei in the Rh matrix served as a source. The Mössbauer spectrometer was calibrated using a standard  $\alpha$ -Fe absorber. The measurements were performed in transmission geometry at room temperature. The Mössbauer spectra were processed using the SpectrRelax least-squares fitting program [27].

#### 2.1.1. Chemical analysis

X-ray microprobe analysis confirmed the high purity of sample studied, the mass fractions of constituent oxides are following: (0.3885  $\pm$  0.0067) FeO, (0.0279  $\pm$  0.0010) MgO, (0.0015  $\pm$  0.0005) MnO, (0.0004  $\pm$  0.0004) CaO, (0.0002  $\pm$  0.0002) SrO, (0.2915  $\pm$  0.0035) P<sub>2</sub>O<sub>5</sub> (the uncertainties of experimental values were calculated with 0.95 level of confidence on the basis of 8 determinations).

#### 2.1.2. Thermogravimetric analysis

The resulting thermograms for natural vivianite (Fig. 1) show one stage of the water removal. If the experiment was carried out under an inert atmosphere (in a nitrogen stream) the dehydration of the mineral occurs in the temperature range (393–723) K, the weight loss is 0.288 mass fraction. When vivianite is heated in a stream of air, its dehydration takes place in the temperature interval (343–773) K simultaneously with the oxidation of divalent iron. In this case the weight loss is less and is 0.25 mass fraction.

#### 2.1.3. X-ray diffraction

The resulting X-ray spectrum of studied sample is consistent with the database of the powder diffraction patterns ICDD № 75-1186 [26] [ICDD] and corresponds to mono-mineral phase with monoclinic structure of vivianite. No impurity phases were detected. The unit-cell parameters of vivianite are:  $a = 10.14(5)$ ,  $b = 13.50(5)$ ,  $c = 4.712(8) \text{ \AA}$ ,  $\beta = 104.3(4)^\circ$  and  $V = 625.0 \text{ \AA}^3$ . These results are in a good agreement with the reference data for natural vivianite from different deposits [28].

#### 2.1.4. FTIR spectroscopy

The IR-absorption spectrum of sample studied (Fig. 2) was analogous to spectrum of vivianite from Eltigen-Ortel deposit (Kerch iron-ore basin, Crimea, Ukraine) [29]. The sample did not contain impurities in the noticeable amounts, and it was the monomineral phase. The absorption spectrum may be divided into three spectral regions.

The first region (3800–2600 cm<sup>-1</sup>) contains a strong sharp band near 3480 cm<sup>-1</sup>, corresponding to valence vibrations of OH-groups in the coordination Fe<sup>3+</sup>OH. The presence of this band confirms the partial oxidation of studied vivianite [8]. A broad absorption band with maximum at 3140 cm<sup>-1</sup> and shoulder near 3300 cm<sup>-1</sup> relate to valence vibrations of OH-groups.

The second area (1700–1500 cm<sup>-1</sup>) contains the absorption band with maximum at 1618 cm<sup>-1</sup> and shoulder near 1663 cm<sup>-1</sup>,

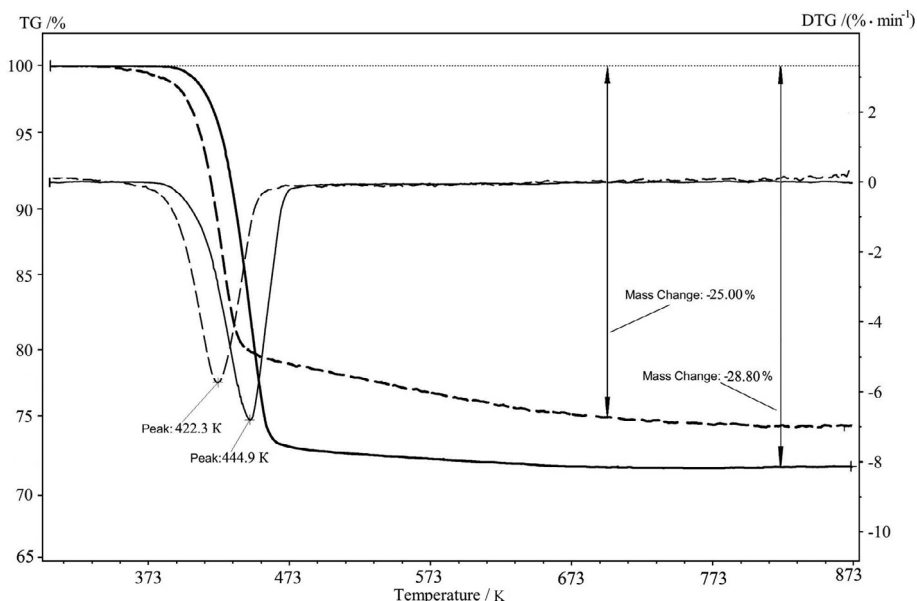


Fig. 1. TG and DTG curves of natural vivianite; full line relates to experiment in nitrogen flow; dotted line – in air flow.

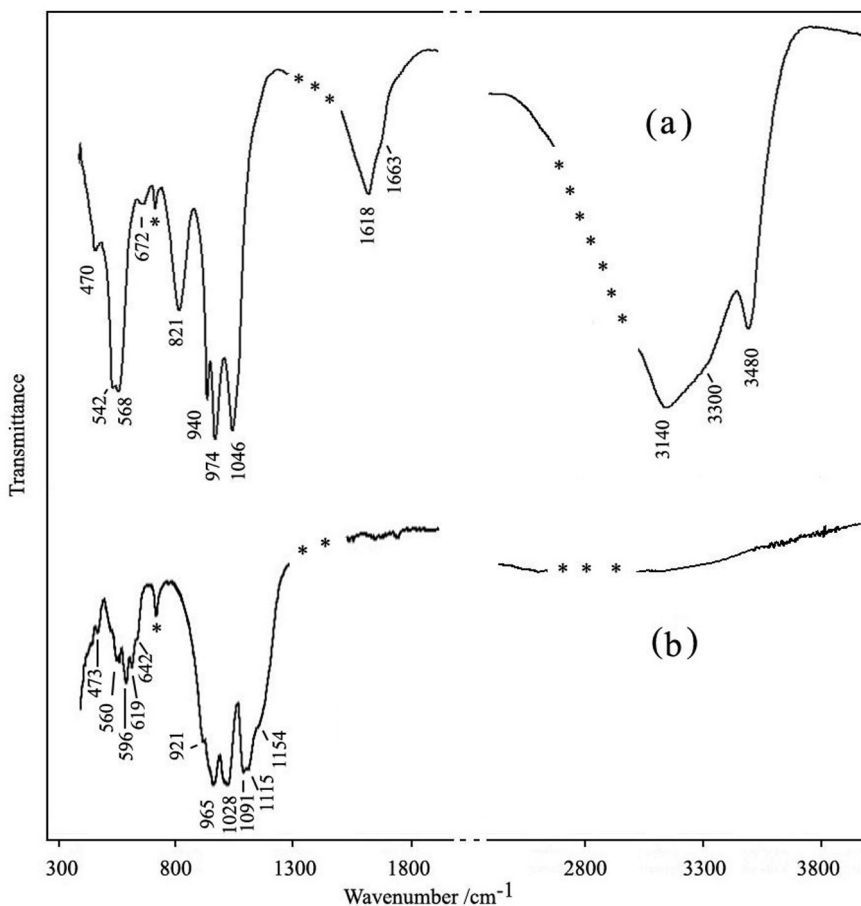


Fig. 2. FTIR spectra of vivianite (obtained in transmission mode): (a) natural sample; (b) after heating up to  $T = 973$  K; \* the absorption band of petrolatum oil.

which corresponds to deformation vibrations of  $H_2O$  molecules and confirms the presence of water in structure in the molecular form.

The third area ( $1200\text{--}400\text{ cm}^{-1}$ ) is the richest by the number of the absorption bands. Two very strong absorption bands near  $1046$  and  $974\text{ cm}^{-1}$  correspond to the triply degenerate valence

vibration  $F_2^{(2)}(v_3)$  of the distorted tetrahedra  $[\text{PO}_4]^{3-}$ . More weak band near  $940\text{ cm}^{-1}$  is associated with totally symmetric valence vibration  $A_1(v_1)$  of tetrahedra  $[\text{PO}_4]^{3-}$ . The intensive band at  $821\text{ cm}^{-1}$  corresponds to the librations of  $\text{H}_2\text{O}$  molecules. The weak band near  $672\text{ cm}^{-1}$  and the strong absorption band with two maxima at  $568$  and  $542\text{ cm}^{-1}$  are associated with the splitting triply degenerate bending vibration  $F_2^{(1)}(v_4)$  of the tetrahedra  $[\text{PO}_4]^{3-}$ . The weak band at  $470\text{ cm}^{-1}$  corresponds to deformation vibration  $E(v_2)$  of the tetrahedra  $[\text{PO}_4]^{3-}$ . No impurity phases were detected.

### 2.1.5. Raman-spectroscopy

The Raman spectrum of studied sample (Fig. 3) is similar to the spectra shown in [6,8,9].

Anion  $[\text{PO}_4]^{3-}$  is manifested in the spectrum by a group of lines: a strong line at  $950\text{ cm}^{-1}$  corresponds to the totally symmetric valence vibration of the anion; a weak line at  $1055\text{ cm}^{-1}$  relates to the triply degenerate antisymmetric valence vibration; the lines at  $539$  and  $572\text{ cm}^{-1}$  belong to the triply degenerate deformation vibration; a line near  $458\text{ cm}^{-1}$  corresponds to doubly degenerate deformation vibration of tetrahedra  $[\text{PO}_4]^{3-}$ . The high-frequency line with maximum at  $3138\text{ cm}^{-1}$  and shoulder near  $3280\text{ cm}^{-1}$  correspond to the valence vibrations of OH-groups (in water molecules). A weak line with maximum near  $3475\text{ cm}^{-1}$  relates to valence vibrations of OH-groups in the coordination  $\text{Fe}^{3+}\text{OH}$  [9]. No impurity phases were detected.

### 2.1.6. Mössbauer spectroscopy

Mössbauer spectrum of studied vivianite (Fig. 4) is easily resolved into four quadrupole doublets.

The hyperfine parameters of the spectrum (Table 2) allow to assign these quadrupole doublets to two different crystallographic non-equivalent positions (A and B), occupied by  $\text{Fe}^{2+}$  and  $\text{Fe}^{3+}$  ions.

The values of the isomer shift and quadrupole splitting for sub-spectra of  $\text{Fe}^{2+}$  ions in “A” position (b in Fig. 4 and Table 2) and “B” position (a in Fig. 4 and Table 2) are in a good agreement with the previous published data [15,30]. The average distance between the iron atom and the nearest oxygen atoms, as well as the degree of distortion of the oxygen octahedron for the position “A”, are considerably greater than for the position “B”. The quadrupole doublet with large values of the isomer shift and quadrupole splitting can be attributed to  $\text{Fe}^{3+}$  ions in “A” position (c in Fig. 4 and Table 2), and the quadrupole doublet with lower values of the isomer shift

and quadrupole splitting can be attributed to  $\text{Fe}^{3+}$  ions in “B” position (d in Fig. 4 and Table 2). Atomic ratios for  $\text{Fe}^{2+}$  and  $\text{Fe}^{3+}$  ions in two distinct interesting for us iron positions were estimated from the relative intensities of the fitted spectral components (Table 2) with the assumption of equal recoil-free fractions for all iron ions  $\text{Fe}_A^{2+}$ ,  $\text{Fe}_B^{2+}$ ,  $\text{Fe}_A^{3+}$ ,  $\text{Fe}_B^{3+}$  (uncertainties were calculated with 0.95 level of confidence):

$$\begin{aligned} \text{Fe}_B^{2+}/\text{Fe}_A^{2+} &= 1.60 \pm 0.02, \quad \text{Fe}_B^{3+}/\text{Fe}_A^{3+} = 0.98 \pm 0.13, \quad \text{Fe}^{3+}/\sum \text{Fe} \\ &= 0.120 \pm 0.004, \end{aligned}$$

Considering the data of X-ray microprobe and thermogravimetric analyses, and results of the Mössbauer spectroscopy, the chemical formula of the studied mineral was calculated on the bases of three cations per formula unit. The obtained formula has the form:  $\text{Fe}_{2.32}^{2+}\text{Fe}_{0.33}^{3+}\text{Mg}_{0.35}(\text{PO}_4)_2(\text{OH})_{0.33}\cdot 7.67\text{H}_2\text{O}$  in accordance with the recommendations of the International Mineralogical Association [20]

### 2.2. Thermochemical methods

The thermochemical studies were carried out using a high-temperature heat-flux Tian-Calvet microcalorimeter (Setaram, France) and differential scanning calorimeter NETZSCH DSC 204 F1 (Germany) at the ambient pressure of  $992 \pm 12\text{ hPa}$ .

#### 2.2.1. Tian-Calvet microcalorimetry

We have performed the thermochemical investigations on a Tian-Calvet microcalorimeter using two different techniques to study natural vivianite containing divalent iron. Character of oxidation process of  $\text{Fe}^{2+}$  and the change of structure and composition of vivianite were early investigated on heating by various methods [14,15,17,18]. The process of simultaneous dehydration and oxidation of vivianite has been studied in present work by a “double drop” method described in [31]. Initially samples of vivianite weighing  $3\text{--}10 (\pm 2 \times 10^{-3})\text{ mg}$  were dropped from room temperature into the empty platinum test-tube, which is in the calorimeter at the temperature  $973\text{ K}$ . This temperature corresponded to completion of the process of total removal of water and total oxidation of  $\text{Fe}^{2+}$  in accordance with our thermal analysis data (Fig. 1). IR absorption spectrum of the sample of vivianite calcinated at  $973\text{ K}$  confirmed a complete dehydration of the substance and

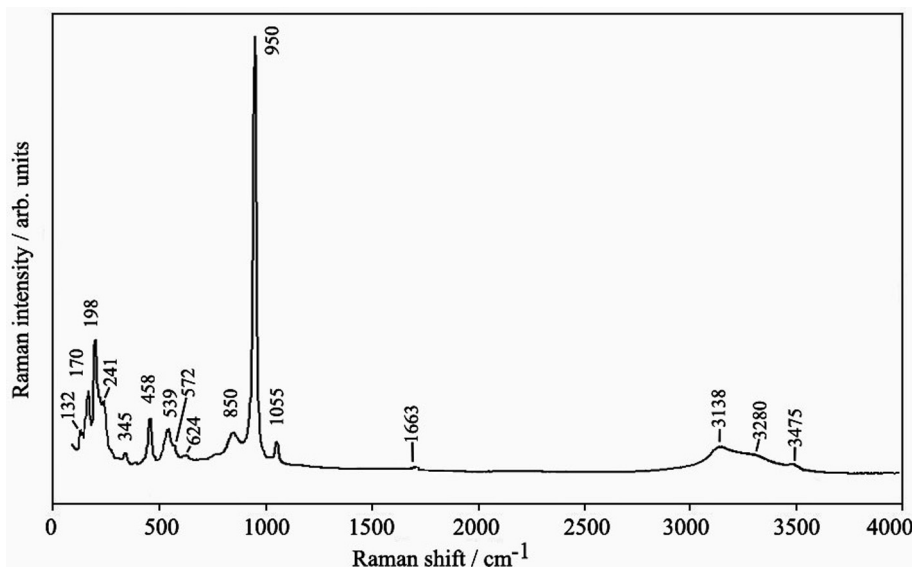


Fig. 3. Raman spectra of natural vivianite (non-oriented sample).

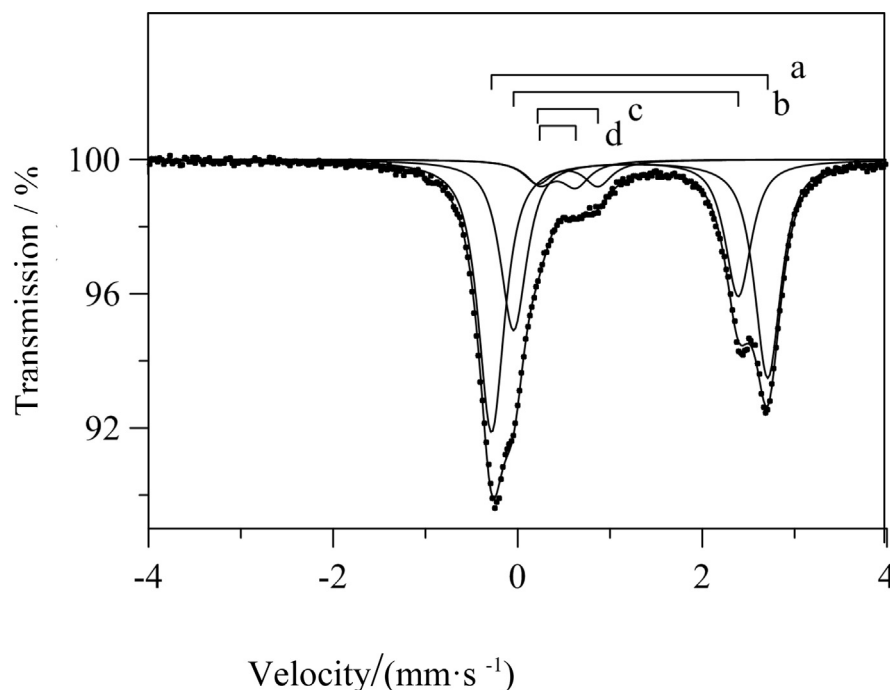


Fig. 4. Mössbauer spectrum of natural vivianite.

Table 2

Mössbauer spectrum parameters of vivianite. The uncertainties were calculated with 0.95 level of confidence.

Quadrupole doublet	Isomer shift/mm s <sup>-1</sup>	Quadrupole splitting/mm s <sup>-1</sup>	Line width/mm s <sup>-1</sup>	Relative intensity/%	Assignment
a	1.212 ± 0.002	2.993 ± 0.002	0.339 ± 0.002	54.1 ± 0.3	Fe <sup>2+</sup> at B
b	1.172 ± 0.002	2.435 ± 0.003		33.9 ± 0.3	Fe <sup>2+</sup> at A
c	0.542 ± 0.050	0.654 ± 0.099	0.363 ± 0.036	6.1 ± 0.5	Fe <sup>3+</sup> at A
d	0.433 ± 0.060	0.392 ± 0.099		6.0 ± 0.4	Fe <sup>3+</sup> at B

registered change of its crystal structure and formation of amorphous phase (Fig. 2b). In [32] the formation of the amorphous phase containing trivalent iron was found at temperatures above 773 K; moreover in [32] it was shown that further increase of temperature above  $T = 923$  K resulted to the formation of the mixture of phases containing phosphates of trivalent iron. In our calorimetric experiment we measured the total heat effect, which includes in addition to the enthalpy increment also enthalpies of dehydration and oxidation of vivianite [ $H^0(T = 973 \text{ K}) - H^0(T = 298.15 \text{ K}) + \Delta_{\text{dehyd.}}H^0(T = 973 \text{ K}) + \Delta_{\text{oxid.}}H^0(T = 973 \text{ K})$ ]. Then, the dehydrated and oxidized sample was dropped again into the calorimeter at the same temperature, and we measured only the value of its enthalpy increment [ $H^0(T = 973 \text{ K}) - H^0(T = 298.15 \text{ K})$ ]. The sample weight was controlled before and after experiment.

The enthalpies of formation of the natural vivianite and its dehydrated and oxidized product were determined by the melt solution calorimetry based on a thermochemical cycle including the dissolution of the substance and its constituent components. We used the melt with composition  $2\text{PbO} \cdot \text{B}_2\text{O}_3$  as a solvent; it was prepared by melting of stoichiometric amounts of lead oxide and boric acid at  $T = 1073 \text{ K}$  (weight accuracy was  $\pm 2 \times 10^{-1} \text{ mg}$ ). The dissolution was carried out by dropping the samples from room temperature into the melt-solvent at  $T = 973 \text{ K}$ . In the experiments the heating of vivianite from room temperature to the temperature of dissolution and its dissolution were carried out in the air and therefore these processes occurred with oxidation of the Fe<sup>2+</sup> containing in the sample. Thus, we measured in this case the value  $\Delta H$ , which consist of the heat content of vivianite [ $H^0(T = 973 \text{ K}) - H^0(T = 298.15 \text{ K})$ ], the enthalpy of its

solution  $\Delta_{\text{sol.}}H^0(T = 973 \text{ K})$  and also enthalpy of its oxidation  $\Delta_{\text{oxid.}}H^0(T = 973 \text{ K})$ . During the dissolution of dehydrated and oxidized sample the value of thermal effect was the sum of heat content and the enthalpy of solution [ $H^0(T = 973 \text{ K}) - H^0(T = 298.15 \text{ K}) + \Delta_{\text{sol.}}H^0(T = 973 \text{ K})$ ]. Masses of the samples for dissolution were (3–8) ( $\pm 2 \times 10^{-3}$ ) mg. When using (30–35) g of solvent during the (6–8) solution experiments the ratio of dissolved substance – melt can be attributed to an infinitely dilute solution with the enthalpy of mixing close to zero. The substances dissolved readily and gave a complete reaction within 30–50 min before a steady baseline signal was restored.

The calibration of the device was carried out on each week of thermochemical studies using the reference substances: platinum (in the experiments on dissolution) and corundum  $\alpha\text{-Al}_2\text{O}_3$  (when studying dehydration and oxidation processes). The necessary data on their enthalpy increments were borrowed from Ref. [33]. The average values of calibration constants obtained were used in calculations.

### 2.2.2. Differential scanning calorimetry

Measurements of the thermal effects of the dehydration and oxidation of natural vivianite were performed with the help of a thermoanalytical system NETZSCH DSC 204 F1 under nitrogen flow (20 ml/min) with a heating rate of 10 K/min in the range from room temperature to 673 K. The device was calibrated using the temperature and the enthalpy of phase transition of standard substances ( $\text{C}_6\text{H}_{12}$ , Hg, Ga,  $\text{KNO}_3$ , In, Sn, Bi, 99.999% purity). Calibration procedure is described in Ref. [34]. Specimens with weights (3–7) ( $\pm 2 \times 10^{-2}$ ) in DSC experiments were tested in standard aluminum



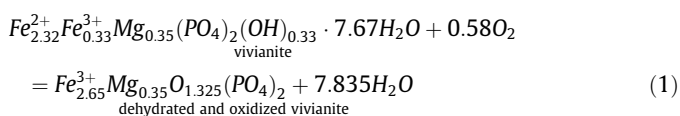
crucibles ( $V = 56 \text{ mm}^3$ ,  $d = 6 \text{ mm}$ ) with pierced lid (ratio of the orifice area to the area of the bottom crucible was about  $2.6 \times 10^{-2}$ ). NETZSCH Proteus Analysis software was applied to process DSC curves. Experimental and computational procedures were performed according to standards ISO 11358 and ISO 11357-1.

Thermoanalytical system NETZSCH is located at the Chemistry Faculty of M.V. Lomonosov Moscow State University, Mössbauer spectrometer MS1104Em is located at the Physical Faculty of M. V. Lomonosov Moscow State University, all other used equipment is located at the Geological Faculty of M.V. Lomonosov Moscow State University.

### 3. Results and discussion

#### 3.1. The enthalpy of dehydration and oxidation of natural vivianite

Using the experimental data on dehydration and oxidation process for vivianite obtained on the Tian-Calvet microcalorimeter (Tables 3 and 4) we calculated the enthalpy of reaction (1) according to Eq. (2). The value of weight loss observed in the experiments (25.00 wt%) corresponds to the removal of all water and total oxidation of divalent iron.



$$\begin{aligned} \Delta_{r(1)}H^0(T = 298.15 \text{ K}) &= [H^0(T = 973 \text{ K}) - H^0(T = 298.15 \text{ K}) \\ &+ \Delta_{\text{dehyd.}}H^0(T = 973 \text{ K}) + \Delta_{\text{oxid.}}H^0(T = 973 \text{ K})] \text{vivanite} + 0.58[H^0(T = 973 \text{ K}) \\ &- H^0(T = 298.15 \text{ K})\text{O}_2 - [H^0(T = 630 \text{ K}) \\ &- H^0(T = 298.15 \text{ K})\text{dehydrated and oxidized vivianite} - 7.835[H^0(T = 630 \text{ K}) \\ &- H^0(T = 298.15 \text{ K})\text{H}_2\text{O}(l)] \end{aligned} \quad (2)$$

where thermochemical data for vivianite and dehydrated and oxidized vivianite are presented in Tables 3 and 4, the reference data for oxygen and water are given from Ref. [33]. The calculated value of the enthalpy of the reaction (1) was found as  $-(70.2 \pm 9.1) \text{ kJ}$ .

The DSC results of vivianite study in the heating mode under flow of nitrogen and air are given in Fig. 5.

During the experiment in an inert atmosphere the measured thermal effect relates to the enthalpy of water removal in the

**Table 3**

Results of Calvet microcalorimeter measurements ( $\text{kJ mol}^{-1}$ ) for natural vivianite.  $\text{Fe}_{2.32}^{2+}\text{Fe}_{0.33}^{3+}\text{Mg}_{0.35}(\text{PO}_4)_2(\text{OH})_{0.33} \cdot 7.67\text{H}_2\text{O}$  (formula weight<sup>a</sup> = 490.23 g) (ambient pressure,  $P = 992 \pm 12 \text{ hPa}$ , the uncertainty is presented as 0.95 confidence interval).<sup>b</sup>

Mass of sample/mg	$H^0(T = 973 \text{ K}) - H^0(T = 298.15 \text{ K}) + \Delta_{\text{dehyd.}}H^0(T = 973 \text{ K}) + \Delta_{\text{oxid.}}H^0(T = 973 \text{ K})$	Mass of sample/mg	$H^0(T = 973 \text{ K}) - H^0(T = 298.15 \text{ K}) + \Delta_{\text{sol.}}H^0(T = 973 \text{ K}) + \Delta_{\text{oxid.}}H^0(T = 973 \text{ K})$
3.012	669.37	3.401	557.19
9.081	653.87	3.572	555.22
10.134	651.73	6.505	562.48
6.903	664.82	7.714	575.06
8.869	661.62	3.971	580.78
8.538	643.53	6.863	563.18
5.971	647.25		Mean value: $565.7 \pm 10.8^c$
	Mean value: $656.0 \pm 8.6^c$		

<sup>a</sup> The values of the formula weight were calculated using necessary data taken from the reference book [33].

<sup>b</sup> The accuracy of determination of calorimetric experiment temperatures was  $\pm 1 \text{ K}$ .

<sup>c</sup> The uncertainty of experimental data was calculated with 0.95 level of confidence.

**Table 4**

Results of Calvet microcalorimeter measurements ( $\text{kJ mol}^{-1}$ ) for dehydrated and oxidized vivianite  $\text{Fe}_{2.65}^{3+}\text{Mg}_{0.35}\text{O}_{1.325}(\text{PO}_4)_2$  (formula weight<sup>a</sup> = 367.64 g) (ambient pressure  $P = 992 \pm 12 \text{ hPa}$ , the uncertainty is presented as 0.95 confidence interval).<sup>b</sup>

Mass of sample/mg	$H^0(T = 973 \text{ K}) - H^0(T = 298.15 \text{ K})$	Mass of sample/mg	$H^0(T = 973 \text{ K}) - H^0(T = 298.15 \text{ K}) + \Delta_{\text{sol.}}H^0(T = 973 \text{ K})$
6.481	202.15	3.583	147.92
7.373	200.64	4.331	136.50
5.389	197.82	5.574	134.60
6.590	199.67	3.135	137.61
6.062	196.30	6.041	139.91
6.478	196.65	3.839	139.84
5.331	194.23	6.173	131.93
6.490	204.40	3.758	135.60
	Mean value: $198.9 \pm 2.9^c$		Mean value: $138.0 \pm 4.1^c$

<sup>a</sup> The values of the formula weight were calculated using necessary data taken from the reference book [33].

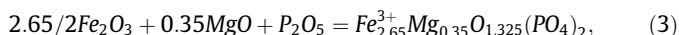
<sup>b</sup> The accuracy of determination of calorimetric experiment temperatures was  $\pm 1 \text{ K}$ .

<sup>c</sup> The uncertainty of experimental data was calculated with 0.95 level of confidence.

temperature range (350–550) K. This value is equal to (408)  $\text{kJ mol}^{-1}$ . In carrying out an experiment under oxidative conditions the measured heat effect in addition includes the enthalpy of mineral oxidation. The value of total heat effect is found to be (187)  $\text{kJ mol}^{-1}$ . The errors of the determination of these values are about 5% in accordance with the accuracy of the instrument calibration constants. Based on these data the enthalpy of vivianite oxidation is evaluated as about  $-(221) \text{ kJ mol}^{-1}$ .

#### 3.2. The enthalpy of formation of natural vivianite

On the basis of the experimental data on the dissolution of the dehydrated and oxidized vivianite (Tables 3 and 4), the value of its standard molar enthalpy of formation from the elements was calculated in accordance with Hess's law using the reaction (3) and Eqs. (4), (5).



$$\Delta_{r(3)}H^0(T = 298.15 \text{ K}) = \sum v_i H_i, \quad (4)$$

$$\Delta_f H_m^0(T = 298.15 \text{ K}) = \Delta_{r(3)}H^0(T = 298.15 \text{ K}) + \sum v_i \Delta_f H_m^0(T = 298.15 \text{ K}), \quad (5)$$

where  $v_i$  is the stoichiometric coefficients in the reaction (3),  $\Delta H = [H^0(T = 973 \text{ K}) - H^0(T = 298.15 \text{ K}) + \Delta_{\text{sol.}}H^0(T = 973 \text{ K})]$  are the thermochemical data for dehydrated and oxidized vivianite (Tables 3 and 4) and constituent oxides (Table 5), the needed for the calculations values of  $\Delta_f H_m^0(T = 298.15 \text{ K})$  of the components of this reaction are also shown in the Table 5. The enthalpy of mixing for an infinitely dilute solution is close to zero. The derived value of  $\Delta_f H_m^0(T = 298.15 \text{ K})$  is equal to:  $-(3034.2 \pm 5.3) \text{ kJ mol}^{-1}$  and relates to the substance of chemical composition  $\text{Fe}_{2.65}^{3+}\text{Mg}_{0.35}\text{O}_{1.325}(\text{PO}_4)_2$ . The value of standard enthalpy of formation for the studied natural vivianite was determined using the above enthalpy of formation of dehydrated and oxidized phase and the obtained value of enthalpy of reaction (1) given at the end of the previous paragraph. The calculation was made on the basis of the Eq. (6).

$$\begin{aligned} \Delta_f H_m^0(T = 298.15 \text{ K})\text{Fe}_{2.32}^{2+}\text{Fe}_{0.33}^{3+}\text{Mg}_{0.35}(\text{PO}_4)_2(\text{OH})_{0.33} \\ \cdot 7.67\text{H}_2\text{O} = \Delta_f H_m^0(T = 298.15 \text{ K})\text{Fe}_{2.65}^{3+}\text{Mg}_{0.35}\text{O}_{1.325}(\text{PO}_4)_2 \\ - \Delta_{r(1)}H^0(T = 298.15 \text{ K}) + 8\Delta_f H_m^0(T = 298.15 \text{ K})\text{H}_2\text{O}(l) \end{aligned} \quad (6)$$

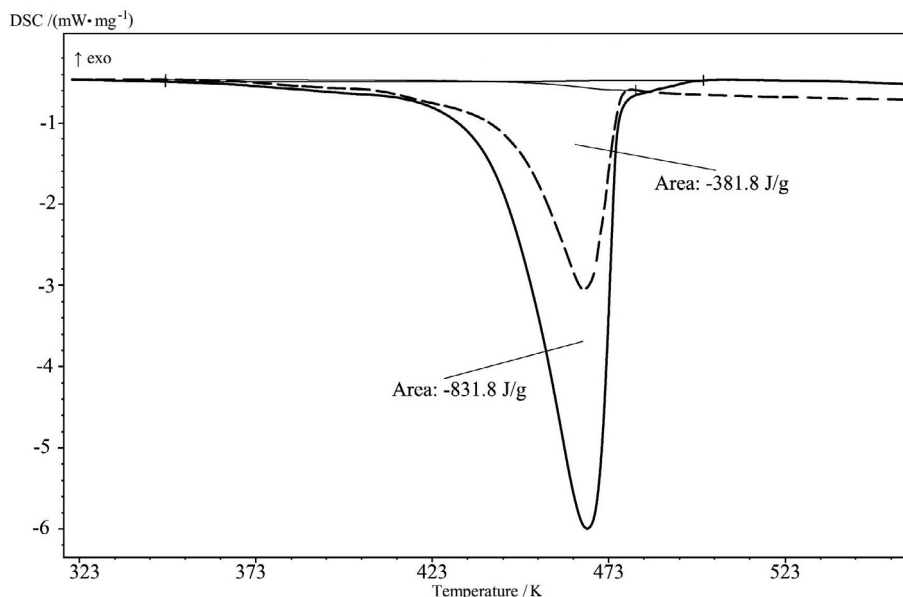


Fig. 5. DSC curves of natural vivianite; full line relates to experiment in nitrogen flow; dotted line – in air flow.

Table 5

Thermochemical data used in the calculation of the standard enthalpies of formation of vivianite.

Component	$\Delta H^{\circ}/\text{kJ mol}^{-1}$	$-\Delta_f H^{\circ}(298.15 \text{ K})^b/\text{kJ mol}^{-1}$
MgO(periclase)	$36.38 \pm 0.59^c$	$601.6 \pm 0.3$
Fe <sub>2</sub> O <sub>3</sub> (hematite)	$171.6 \pm 1.9^d$	$826.2 \pm 1.3$
Al <sub>2</sub> O <sub>3</sub> (corund)	$107.38 \pm 0.59^e$	$1675.7 \pm 1.3$
Al(OH) <sub>3</sub> (gibbsite)	$172.6 \pm 1.9^f$	$1293.1 \pm 1.2$
P <sub>2</sub> O <sub>5</sub> (s)	$-326.5 \pm 1.2^g$	$1504.9 \pm 0.5$

<sup>a</sup>  $\Delta H = [H^{\circ}(973 \text{ K}) - H^{\circ}(298.15 \text{ K}) + \Delta_{\text{sol}} H^{\circ}(973 \text{ K})]$ .

<sup>b</sup> The values of  $\Delta_f H_m^{\circ}(298.15 \text{ K})$  are the reference data from Ref. [33].

<sup>c</sup> The value of  $\Delta H$  was calculated using reference data on  $[H^{\circ}(973 \text{ K}) - H^{\circ}(298.15 \text{ K})]$  [33] and experimental data on  $\Delta_{\text{sol}} H^{\circ}(973 \text{ K})$  from Ref. [35].

<sup>d</sup> The value of  $\Delta H$  was calculated using reference data on  $[H^{\circ}(973 \text{ K}) - H^{\circ}(298.15 \text{ K})]$  [33] and experimental data on  $\Delta_{\text{sol}} H^{\circ}(973 \text{ K})$  from Ref. [36].

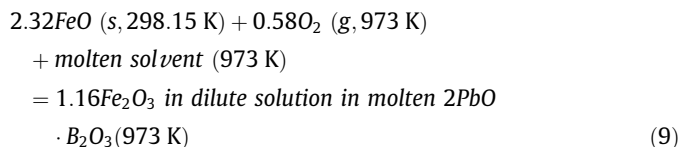
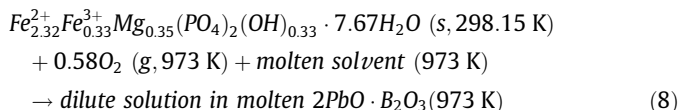
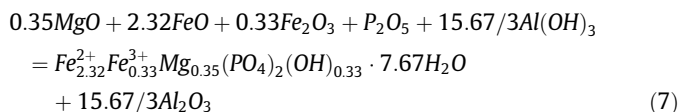
<sup>e</sup> The value of  $\Delta H$  was calculated using reference data on  $[H^{\circ}(973 \text{ K}) - H^{\circ}(298.15 \text{ K})]$  [33] and experimental data on  $\Delta_{\text{sol}} H^{\circ}(973 \text{ K})$  from Ref. [37].

<sup>f</sup> The value of  $\Delta H$  is the experimental data from Ref. [38].

<sup>g</sup> The value of  $\Delta H$  is the experimental data from Ref. [39].

The value of  $\Delta_f H_m^{\circ}(T = 298.15 \text{ K})$  of vivianite studied was calculated as  $-(5203 \pm 11) \text{ kJ mol}^{-1}$ .

The enthalpy of formation of vivianite was also determined using the data on dissolution of natural mineral given the fact that oxidation of divalent iron present in mineral composition occurs during dissolution. The thermochemical cycle, which was used to determine the enthalpy of formation of  $\text{Fe}_{2.65}^{3+}\text{Mg}_{0.35}\text{O}_{1.325}(\text{PO}_4)_2$ , cannot be applied for vivianite, it must be supplemented by reactions, associated with oxidation processes. The value of  $\Delta_f H_m^{\circ}(T = 298.15 \text{ K})$  vivianite was calculated on the basis of the reaction (7) and additional oxidation reactions (8), (9).



The calculation of  $\Delta_f H_m^{\circ}(298.15 \text{ K})$  for natural vivianite was made according to the equation:

$$\Delta_f H_m^{\circ}(T = 298.15 \text{ K}) \text{ vivianite} \\ = \sum v_i \Delta_f H_i - \Delta_{r(8)} H^{\circ} + \Delta_{r(9)} H^{\circ} + \sum v_i \Delta_f H_m^{\circ}(T = 298.15 \text{ K}), \quad (10)$$

where  $v_i$  is the stoichiometric coefficients in the reaction (7),  $\Delta_f H_i$  is the heat of drop solution  $[H^{\circ}(T = 973 \text{ K}) - H^{\circ}(T = 298.15 \text{ K}) + \Delta_{\text{sol}} H^{\circ}(T = 973 \text{ K})]$  of components of reaction (7) except iron oxide under the same calorimetric conditions,  $\Delta_f H_m^{\circ}(298.15 \text{ K})_i$  is the standard enthalpy of formation for all oxides and aluminum hydroxide (Table 5). The value of the enthalpy of the reaction (8) was obtained experimentally in this work (Tables 3 and 4), the value of the enthalpy of reaction (9), which is equal to  $-(140.4 \pm 3.6) \text{ kJ}$ , was calculated using reference data [33] on the enthalpy increment of FeO (s) at  $T = 973 \text{ K}$ , standard enthalpies of formation of FeO(s) and Fe<sub>2</sub>O<sub>3</sub>(s) at  $T = 973 \text{ K}$ , and the enthalpy of solution of Fe<sub>2</sub>O<sub>3</sub>(s) [35]. The found standard molar enthalpy of formation of natural vivianite from the elements at  $T = 298.15 \text{ K}$  is equal to  $-(5231 \pm 18) \text{ kJ mol}^{-1}$ . The values obtained by the two methods agree with each other within given errors. The average value (Table 6) can be recommended as the standard enthalpy of formation of studied vivianite.

Table 6

Thermodynamic properties of vivianite at  $T = 298.15 \text{ K}$ . The errors are calculated on the basis of the law of propagation of uncertainty.

Composition of mineral	$-\Delta_f H_m^{\circ}/\text{kJ mol}^{-1}$	$S_m^{\circ}/\text{J}(\text{K mol})^{-1}$	$-\Delta_f G_m^{\circ}/\text{kJ mol}^{-1}$
$\text{Fe}_{2.32}^{2+}\text{Fe}_{0.33}^{3+}\text{Mg}_{0.35}(\text{PO}_4)_2(\text{OH})_{0.33} \cdot 7.67\text{H}_2\text{O}$	$5217 \pm 11$	558.0	$4540 \pm 11$
$\text{Fe}_3^{2+}(\text{PO}_4)_2 \cdot 8\text{H}_2\text{O}$	$5119 \pm 19$	571.0	$4439 \pm 19$

### 3.3. The Gibbs energy of formation of natural vivianite

No value of the standard entropy of studied vivianite needed to calculate its Gibbs energy is currently available from the literature. We evaluated this value on the basis of additivity employing the averaged entropy values attributable to the cations and anions in the solids (Latimer method). Necessary for calculation data on the entropies of water, cations and anions were taken from Ref. [40]. Using the estimated value of  $S^0$  ( $T = 298.15$  K) (Table 6) and obtained in the present work value of  $\Delta_f H_m^0$  ( $T = 298.15$  K) of vivianite we calculated the value of Gibbs energy of formation from the elements for this natural mineral (Table 6).

### 3.4. The thermodynamic properties of vivianite of theoretical composition

The enthalpy of formation of vivianite of the theoretical composition  $\text{Fe}_3^{2+}(\text{PO}_4)_2 \cdot 8\text{H}_2\text{O}$  (Table 6) was calculated on the basis of the dissolution calorimetric data for the natural mineral. For this purpose, the results of the measurements for studied vivianite were corrected on the deviations of its composition from the ideal formula; the amendments were estimated using the thermochemical data for the corresponding components (Table 5). The calculation of the value of  $\Delta_f H_m^0$  ( $T = 298.15$  K) vivianite was made using equations analogous (7, 8, 9). The values of the standard entropy and Gibbs energy were calculated by the same way as for the natural mineral and are given in the Table 6. The obtained data on  $\Delta_f G_m^0$  ( $T = 298.15$  K) vivianite confirm an estimate of this value ( $-4428.2$  kJ mol<sup>-1</sup>) presented in Ref. [22].

### 3.5. Conclusion

Our new experimental data complement the modern base of thermodynamic constants of phosphate minerals needed for modeling the processes of formation of phosphates in different geological environments. Phosphates due to their varying degrees of oxidation and dehydration can serve as indicators of degree of oxidation, acidic/alkaline and hydrated/dehydrated conditions of formation of mineral assemblages [13].

## References

- [1] H. Mori, T. Ito, The structure of vivianite and symplectite, *Acta Crystallogr.* 3 (1950) 1–6.
- [2] P. Fejdi, J.F. Poullen, M. Gaspérin, Refinement de la structure de la vivianite  $\text{Fe}_3(\text{PO}_4)_2 \cdot 8\text{H}_2\text{O}$ , *Bull. Minér.* 103 (1980) 147–160.
- [3] T. Sameshima, G.S. Henderson, P.M. Black, K.A. Rodgers, X-ray diffraction studies of vivianite, metavivianite, and baricite, *Miner. Mag.* 49 (1985) 81–85.
- [4] D. Rouzies, J.M.M. Millet, Mössbauer study of synthetic oxidized vivianite at room temperature, *Hyperfine Interact.* 77 (1993) 19–28.
- [5] K.A. Rodgers, H.W. Kobe, C.W. Childs, Characterization of vivianite from Catavi, Llagagua Bolivia, *Mineral. Petrol.* 47 (1993) 193–208.
- [6] R.L. Frost, W. Martens, P.A. Williams, T. Klopogge, Raman and infrared spectroscopic study of the vivianite-group phosphates vivianite, baricite and bobierite, *Miner. Mag.* 66 (6) (2002) 1063–1073.
- [7] R.L. Frost, T. Klopogge, M.L. Weier, W.N. Martens, Z. Ding, H.G.H. Edwards, Raman spectroscopy of selected arsenates—implications for soil remediation, *Spectrochim. Acta A* 59 (2003) 2241–2246.
- [8] R.L. Frost, M. Weier, W.G. Lyon, Metavivianite an intermediate phase between vivianite, and ferro/ferristrunzite – a Raman spectroscopic study, *Neues Jahrb. Mineral. Monatsh.* 5 (2004) 228–240.
- [9] R.L. Frost, M.L. Weier, Raman spectroscopic study of vivianites of different origins, *Neues Jahrb. Mineral. Monatsh.* 10 (2004) 445–463.
- [10] N. Fagel, L.Y. Alleman, L. Granina, F. Hatert, E. Thamo-Bozso, R. Cloots, L. André, Vivianite formation and distribution in Lake Baikal sediments, *Global Planet. Change* 36 (2005) 315–336.
- [11] K.G. Taylor, K.A. Hudson-Edwards, A.J. Bennett, V. Vishnyakov, Early diagenetic vivianite  $[\text{Fe}_3^{2+}(\text{PO}_4)_2 \cdot 8\text{H}_2\text{O}]$  in a contaminated freshwater sediment and insights into zinc uptake: a  $\mu$ -EXAFS,  $\mu$ -XANES and Raman study, *Appl. Geochem.* 23 (2008) 1623–1633.
- [12] W. Jastrzębski, M. Sitarz, M. Rokita, K. Bułat, Infrared spectroscopy of different phosphates structures, *Spectrochim. Acta A* 79 (2011) 722–727.
- [13] M.D. Dyar, E.R. Jawin, E. Breves, G. Marchand, M. Nelms, M.D. Lane, S.A. Mertzman, D.L. Bish, J.L. Bishop, Mössbauer parameters of iron in phosphate minerals: implications for interpretation of martian data, *Am. Mineral.* 99 (2014) 914–942.
- [14] R.L. Frost, M.L. Weier, W. Martens, J.T. Klopogge, Z. Ding, Dehydration of synthetic and natural vivianite, *Thermochim. Acta* 401 (2003) 121–130.
- [15] C.A. McCammon, R.G. Burns, The oxidation mechanism of vivianite as studied by Mössbauer spectroscopy, *Am. Mineral.* 65 (1980) 361–366.
- [16] J.-I. Dormann, J.-F. Poullen, Nude par spectroscopie Mössbauer de vivianites oxydées naturelles, *Bull. Minér.* 103 (1980) 633–639.
- [17] K.A. Rodgers, Metavivianite and kerchenite: review, *Miner. Mag.* 50 (1986) 687–691.
- [18] A.R. Pratt, Vivianite auto-oxidation, *Phys. Chem. Miner.* 25 (1997) 24–27.
- [19] K.A. Rodgers, G.S. Henderson, The thermochemistry of some iron phosphate minerals: vivianite, metavivianite, baricite, ludlamite and vivianite/metavivianite admixtures, *Thermochim. Acta* 104 (1986) 1–12.
- [20] International Mineralogical Association, <<http://www.ima-mineralogy.org>>.
- [21] N.V. Chukanov, R. Scholz, S.M. Aksenov, R.K. Rastsvetaeva, I.V. Pekov, D.I. Belakovskiy, K. Krambrock, R.M. Paniago, A. Richi, R.F. Martins, F.M. Belotti, V. Bermanes, Metavivianite,  $\text{Fe}^{2+}\text{Fe}^{3+}(\text{PO}_4)_2(\text{OH})_2 \cdot 6\text{H}_2\text{O}$ : new data and formula revision, *Miner. Mag.* 76 (3) (2012) 725–741.
- [22] A. Valero, A. Valero, P. Vieillard, The thermodynamic properties of the upper continental crust: exergy, Gibbs free energy and enthalpy, *Energy* 41 (2012) 121–127.
- [23] R.O. Grishchenko, A.L. Emelina, P.Y. Makarov, Thermodynamic properties and thermal behaviour of Friedel's salt, *Thermochim. Acta* 570 (2013) 74–79.
- [24] WinXPow Software, STOE & CIE GmbH, 2002.
- [25] Match! Software, Crystal Impact GbR, 2016.
- [26] The International Centre for Diffraction Data, PDF-2//<[www.icdd.com](http://www.icdd.com)>, 2013.
- [27] M.E. Matsnev, V.S. Rusakov, SpectrRelax – an application for Mössbauer spectra modeling and fitting, *AIP Conf. Proc.* 1489 (2012) 178–185.
- [28] Database of Raman Spectroscopy, X-ray Diffraction and Chemistry Of minerals, <<http://www.ruff.info/>>.
- [29] N.V. Chukanov, *Infrared Spectra of Mineral Species: Extended Library*, Springer-Verlag GmbH, Dordrecht-Heidelberg-New York-London, 2014, p. 1703.
- [30] E. Mattievich, J. Danon, Hydrothermal synthesis and Mössbauer studies of ferrous phosphates of the homologous series  $\text{Fe}_3^{2+}(\text{PO}_4)_2(\text{H}_2\text{O})_n$ , *J. Inorg. Nucl. Chem.* 39 (1977) 569–580.
- [31] I.A. Kiseleva, L.P. Ogorodova, L.V. Melchakova, M.R. Bisengalieva, N.S. Becturganov, Thermodynamic properties of copper carbonates – malachite  $\text{Cu}_2(\text{OH})_2\text{CO}_3$  and azurite  $\text{Cu}_3(\text{OH})_2(\text{CO}_3)_2$ , *Phys. Chem. Miner.* 19 (1992) 322–333.
- [32] M.O. Figueiredo, S. Furtado, J.S. Waerenborgh, Decomposição térmica da vivianite de Mangualde, *Mem. Not. Publ. Mus. Lab. Mineral. Geol. Univ. Coimbra* 98 (1984) 83–90.
- [33] R.A. Robie, B.S. Hemingway, Thermodynamic properties of minerals and related substances at 298.15 K and 1 bar (105 Pascals) pressure and at higher temperatures, *U.S. Geol. Surv. Bull. No.* 2131 (1995) 461.
- [34] D.A. Kosova, A.L. Voskov, N.A. Kovalenko, I.A. Uspenskaya, A water-urea-ammonium sulfamate system: experimental investigation and thermodynamic modeling, *Fluid Phase Equilib.* 425 (2016) 312–323.
- [35] A. Navrotsky, W.J. Coons, Thermochemistry of some pyroxenes and related compounds, *Geochim. Cosmochim. Acta* 40 (1976) 1281–1295.
- [36] I.A. Kiseleva, Thermodynamic properties and stability of pyrope, *Geochem. Int.* 13 (1976) 139–146.
- [37] L.P. Ogorodova, L.V. Melchakova, I.A. Kiseleva, I.A. Belitsky, Thermochemical study of natural pollucite, *Thermochim. Acta* 403 (2003) 251–256.
- [38] L.P. Ogorodova, I.A. Kiseleva, L.V. Mel'chakova, M.F. Viganina, E.M. Spiridinov, Calorimetric determination of the enthalpy of formation for pyrophyllite, *Russ. J. Phys. Chem. A* 85 (9) (2011) 1492–1494.
- [39] S.V. Ushakov, K.V. Helean, A. Navrotsky, L.A. Boatner, Thermochemistry of rare-earth orthophosphates, *J. Mater. Res.* 16 (9) (2001) 2623–2633.
- [40] G.B. Naumov, B.N. Ryzhenko, I.L. Khodakovskii, *A Reference Book of Thermodynamic Values for Geologists*, Moscow, Atomizdat, 1971, 239 (in Russian).